JOURNAL OF GEOPHYSICAL RESEARCH, VOL. 93, NO. A9, PAGES 10,001–10,010, SEPTEMBER 1, 1988

Double-Probe Potential Measurements Near the Spacelab 2 Electron Beam

J. T. STEINBERG[1] AND D. A. GURNETT

Department of Physics and Astronomy, University of Iowa, Iowa City

P. M. BANKS

STAR Laboratory, Stanford University, Stanford, California

W. J. RAITT

Center for Atmospheric and Space Sciences, Utah State University, Logan

As part of the Spacelab 2 mission the plasma diagnostics package (PDP) was released from the shuttle as a free-flying satellite. The PDP carried a quasi-static electric field instrument which made differential voltage measurements between two floating probes. At various times during the free flight, an electron beam was ejected from the shuttle. Large differential voltages between the double probes were recorded in association with the electron beam. However, analysis indicates that these large signals are probably not caused by ambient electric fields. Instead, they can be explained by considering three effects: shadowing of the probes from streaming electrons by the PDP chassis, crossing of the PDP wake by the probes, and spatial gradients in the fluxes of energetic electrons reaching the probes. Plasma measurements on the PDP show that energetic electrons exist in a region 20 m wide and up to at least 170 m downstream from the electron beam. At 80 or more meters downstream from the beam, the double probe measurements show that the energetic electron flux is opposite to the injection direction, as would be expected for a secondary returning electron beam produced by scattering of the primary electron beam.

1. INTRODUCTION

As part of the Spacelab 2 mission, a spacecraft called the plasma diagnostics package (PDP) was released from the shuttle to survey the plasma environment around the orbiter. At various times, an electron beam was ejected from the shuttle so that the effects produced in the plasma might be studied. In this paper we report on efforts to measure the quasi-static electric fields in the plasma with the PDP, focusing on those times when the electron beam generator was operating. The PDP, a scientific instrument package containing 14 instruments, was designed and constructed at the University of Iowa, and is described by *Shawhan* [1982]. The electron beam generator, flown as part of the vehicle charging and potential (VCAP) experiment provided by Stanford University and Utah State University, is described by *Banks et al.* [1987]. The PDP and the electron beam generator were previously flown on the STS-3 flight [*Shawhan et al.*, 1984].

Prior to the shuttle flights, a number of electron beam experiments were performed in plasma chambers and from rockets. Using the same PDP and the same electron beam generator later flown onboard Spacelab 2, quasi-static electric fields of the order of a few volts per meter were measured within a few meters of the beam in a large plasma chamber at Johnson Space Flight Center [*Shawhan*, 1982]. *Denig* [1982] questioned the reliability of these measurements because of the possibility of differential charging on the measuring probes, and because the fields seemed too large to be sustained in the given apparatus. *Kellogg et al.* [1982] also reported measuring fields of a few volts/m in a similar chamber test. Measurements of the quasi-static electric fields have also been reported in association with electron beams emitted from rockets in the ionosphere. In the Polar 5 experiment, fields of the order of 0.1 V/m were detected over 100 m away from the beam source [*Jacobsen and Maynard*, 1978]. During the Echo 6 experiment, *Winckler and Erickson* [1986] measured fields of the order of 0.2 V/m at a distance of 40 m from the flux tube on which the beam was expected to be centered. All the measurements mentioned here involved differential voltage measurements on floating probes. Considering the chamber and rocket experiments, we expected on the Spacelab 2 mission to detect fields on the order of 1 V/m associated with the electron beam.

The Spacelab 2 mission was launched into a nearly circular orbit, of inclination 49.5°, at a nominal altitude of 325 km. The PDP was in free flight roughly 6 hours, during which the shuttle peformed two complete fly-arounds of the PDP. During the fly-around the shuttle was maneuvered to regions upstream and downstream of the PDP. The fly-around included four magnetic conjunctions during which the shuttle was targeted to pass through the magnetic field line passing through the PDP. The electron beam generator was operated at various times throughout the free flight, both in a steady (dc) mode, and in a pulsed mode. During several of these times large signals were detected by the quasi-static electric field instrument. The purpose of this paper is to describe the large signals associated with the electron beam firings and to determine the origin of these signals.

2. INSTRUMENTATION

The PDP quasi-static electric field instrument made potential measurements on two floating probes. These floating probes consisted of conducting spheres mounted on insulated

[1]Now at Center for Space Research, Massachusetts Institute of Technology, Cambridge.

Paper number 7A9230.
0148-0227/88/007A-9230$05.00

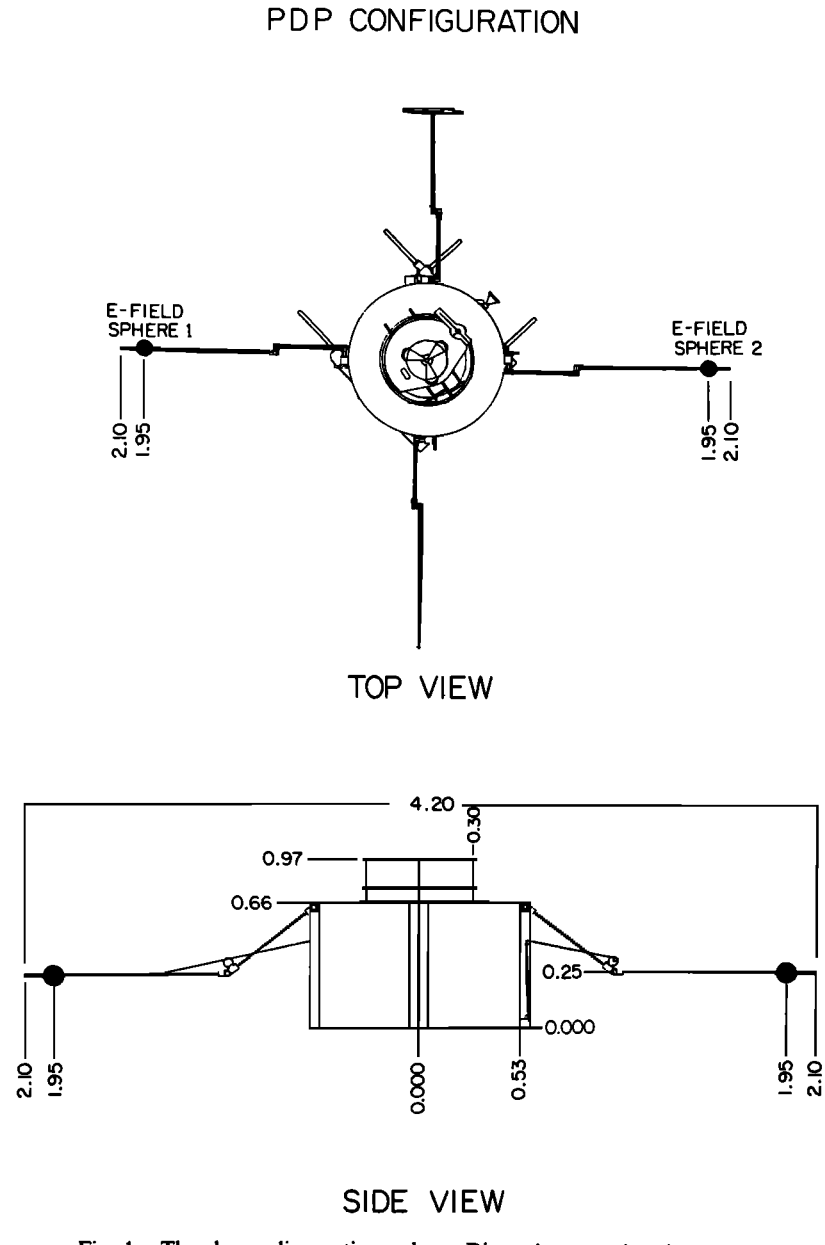

Fig. 1. The plasma diagnostics package. Dimensions are given in meters.

booms on opposite sides of the spacecraft. The sphere-to-sphere separations was 3.89 m, and the diameter of the spheres was 10.2 cm. A diagram of the PDP, showing the dimensions of the main chassis and the locations of spherical probes 1 and 2, is presented in Figure 1. Two types of measurements were made: the differential voltage, V_{diff}, between the two probes was measured at both a high gain and a low gain, and the average potential, V_{ave}, of the two probes relative to the PDP chassis was measured. The following relations describe the two measurements:

$$V_{diff} = V_2 - V_1$$

$$V_{ave} = (V_2 + V_1)/2$$

where V_1 and V_2 are respectively the potentials of sphere 1 and sphere 2 relative to the PDP chassis. Typically, the differential voltage divided by the antenna length is interpreted as a measurement of the electric field. The basic instrument parameters and dynamic ranges are given in Table 1. Since the floating potential of an object in a plasma is dependent on the

TABLE 1. Instrument Parameters and Dynamic Ranges

	Value
Electric field high gain range	± 0.064 V/m
Electric field high gain precision	± 0.51 mV/m
Electric field low gain range	± 2.0 V/m
Electric field low gain precision	± 0.017 V/m
Electric field sample rate	20.0 samples/s
Average potential range	± 8.0 V
Average potential sample interval	1.6 s/sample
Spherical probe separation	3.89 m
Spherical probe diameter	10.2 cm

surface materials, it is also important to describe the surface properties of the spacecraft and spheres. The PDP chassis was covered with a teflon-coated fiberglass cloth which in turn was covered with an aluminum mesh to provide a uniform conducting surface. Potential measurements were referenced to the aluminum mesh. The spherical antenna probes were coated with a conducting graphite-epoxy paint.

After release from the shuttle, the PDP was made to spin by the action of an inertia wheel within the PDP. When spinning at its maximum rate, the spacecraft had a spin period of 13.1 s. The spin axis was oriented approximately perpendicular to the orbital plane. Thus the spacecraft velocity vector lay approximately in the PDP spin plane.

The electron beam generator was mounted in the shuttle payload bay. A beam was produced as electrons emitted from a heated tungsten wire filament were accelerated through a 1-kV potential. The generator operated at beam currents of either 50 mA or 100 mA, producing either a steady or a pulsed beam. The beam was pulsed at frequencies up to 800 kHz.

3. Observations

During most of the free flight, the V_{diff} signals were of the order of the induced potential due to the orbital motion of the spacecraft, $|(\mathbf{V} \times \mathbf{B}) \cdot \mathbf{L}|$, where V is the spacecraft velocity and L is a vector pointing from sphere 2 to sphere 1. These signals were typically 0.4 and 0.8 V. The V_{ave} signal was usually between zero and a few volts positive. That is, the PDP normally floated at a slightly lower potential than the antenna probes. The V_{ave} signal also showed a periodic variation synchronous with the spacecraft spin period. The periodic variation was found to be related to the operation of the PDP low energy proton and electron differential energy analyzer (LEPEDEA) [*Tribble et al.*, 1988]. The LEPEDEA utilized a current collecting plate whose voltage jumped to +2 kilovolts every 1.6 s. The plate collected a large thermal electron current, and the PDP potential decreased by several volts, recovering to its initial value within 1.0 s. The V_{ave} signal was spin modulated because the degree of charging of the spacecraft was less when the LEPEDEA aperture faced the spacecraft wake, than when the aperture faced the ram direction. For the V_{diff} measurement, a large negative potential on the PDP was equivalent to a large positive common mode signal on the probes. Because of limitations in the common mode rejection, the V_{diff} signal was disturbed whenever the PDP potential exceeded several volts negative. The magnitude of the instrument output due to the common mode signal was generally much less than $|(\mathbf{V} \times \mathbf{B}) \cdot \mathbf{L}|$. Thus the common mode signal was large enough to make the interpretation of the measurements difficult when the difference between the V_{diff} and $|(\mathbf{V} \times \mathbf{B}) \cdot \mathbf{L}|$ was small. However, for V_{diff} signals larger than $|(\mathbf{V} \times \mathbf{B}) \cdot \mathbf{L}|$, the common mode rejection problem was not important.

At five times during the free flight when the electron beam generator was operating, V_{diff} signals were recorded that were significantly larger than $|(\mathbf{V} \times \mathbf{B}) \cdot \mathbf{L}|$. The signals for these events are shown in Figure 2, and the events are numbered 1–5. At no other times during the PDP free flight were signals this large recorded. Of these five events, the beam was operated in a steady mode for three events, and in a pulsed mode for two events. The beam injection pitch angle varied widely among the events. Table 2 lists the beam operation mode, injection pitch angle, beam current, and several other important parameters regarding these five events.

The basic periodicity of the V_{diff} signals in Figure 2 is due to the spinning of the spacecraft. In addition to the overall variation at the spin period, the signals have a number of unusual features. During event 1 the instrument saturates. Thus, the difference voltage on the probes is greater than 8 V, which corresponds to an inferred electric field strength in the spin

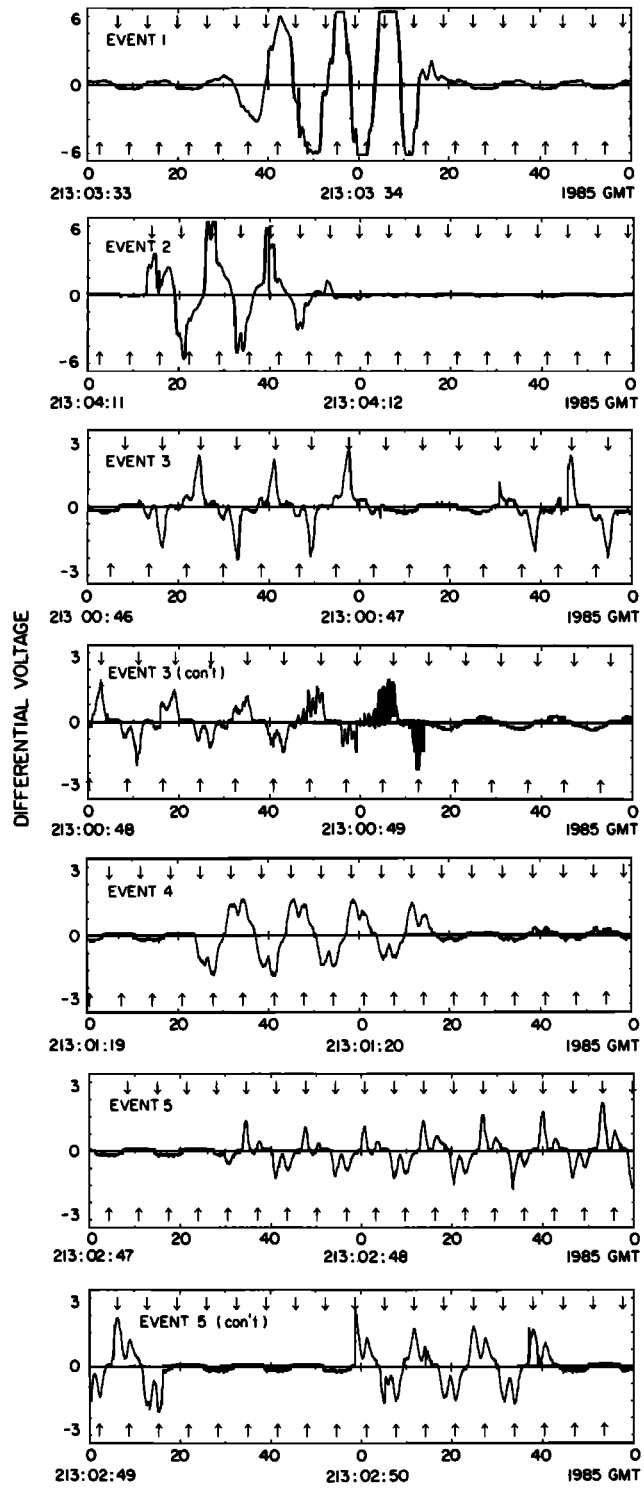

Fig. 2. Large differential voltage signals associated with times of the electron beam generator operation. Arrows at the top indicate times the antenna was aligned with the spacecraft velocity vector. Arrows at the bottom indicate times the antenna was aligned with the magnetic field.

TABLE 2. Beam Parameters, Sunlight Conditions, PDP Orientation

Event	1	2	3	4	5
Distance from PDP to shuttle	206 m	218 m	93 m	90 m	235 m
Distance from PDP to flux tube of beam	26–3 m	9–40 m	87 m	84 m	143 m
Θ, Angle of B to spin plane	22.9°–23.6°	15.4°–15.7°	15.1°–19.4°	10.8°–12.1°	15.4°–16.6°
Day/night	day	night	night	night-sunrise	night-sunrise
Beam current	50 mA	100 mA	100 mA	100 mA	100 mA
Beam injection direction	down	up	down	up	up
Beam injection pitch angle	<7.5°	2.4°–10°	54°–70°	68°–69°	38°–45°
Beam mode	dc	1.2 kHz	54 s dc 115 s pulsed 600 Hz stepped down to 10 Hz	dc	dc

plane greater than 2 V/m. Event 2 has a "spiky" character, and events 3, 4, and 5 all show a "double peak" character. At the end of event 3 (around 0049), there is an apparent higher frequency structure to the signal. This structure is associated with the pulsing of the electron beam. Note that as long as the beam pulse frequency is much greater than the V_{diff} sample rate, then no effect of the pulsing should be apparent in the V_{diff} signal. Such is the case for event 2, where the beam was pulsed at 1.2 kHz. However, during event 3 the beam pulse frequency was lower in steps from 600 Hz down to frequencies near the V_{diff} sample frequency of 20 Hz. The apparent higher frequency structure is the result of a beating effect that occurs between the beam pulse rate and the V_{diff} sample rate.

In order to understand the origin of the large signals, the phase angle of the spinning PDP was investigated. Arrows are plotted in Figure 2 at the top of the graph to indicate the times when the electric antenna was aligned with the spacecraft velocity vector. Recall that the velocity vector lay approximately in the PDP spin plane. Arrows are plotted in Figure 2 at the bottom of the graph to indicate times when the antenna was aligned with the magnetic field projected onto the spin plane. In general, the magnetic field vector did not lie exactly in the spin plane, but made an angle of between 10° and 24° with the spin plane. The angle for each event is given in Table 2. Inspection of Figure 2 reveals that for cases 2, 3, 4, and 5 a voltage peak occurs when the antenna is aligned with the spacecraft velocity vector, and for cases 3, 4, and 5 a second peak occurs when the antenna is aligned parallel to the magnetic field projected onto the spin plane.

Figure 3 shows the trajectory of the PDP in a plane perpendicular to the magnetic field during all times that the electron beam generator was operating. The direction $V_\perp$ indicated in the figure is along the component of the velocity perpendicular to **B**. The origin represents the position of the magnetic field line on which the electron beam should be centered. The beam is assumed to lie on a magnetic field line which intersects the electron beam generator, and the field is determined from a multipole model of the Earth's magnetic field. Although shown in Figure 3 only as a point, the beam will have a cyclotron motion about the magnetic field. The injection pitch angles are listed in Table 2. The pitch angles vary over a large range, but are relatively small (less than 10°) for events 1 and 2, and large (greater than 30°) for events 3, 4, and 5. The beam also has some spreading due to beam divergence, space charge repulsion of the beam electrons, and beam instability. The actual width of the beam is unknown; however, previous beam experiments indicate that the cyclotron radius of a beam electron with pitch angle 90° is a reasonable approximation for the beam radius. For a 1-keV electron in a magnetic field of 0.25–0.5 G, the cyclotron radius is approximately 2–4 m.

The trajectories during the five large events are shown in Figure 3 as solid segments, and the trajectories during times when the beam generator was operating but the measured differential voltage was small (i.e., less than $|\mathbf{V} \times \mathbf{B}|$), are shown by the dashed lines. During events 1 and 2, the length of time the electron beam generator was turned on was longer than the length of time large signals were recorded, indicating that the spatial region over which large signals occur is limited. For each of events 3, 4, and 5, large signals were recorded for the entire period the beam generator was on. Note that events 1–5 occur at times when the PDP was in a region downstream of the flux tube carrying the electron beam. Except briefly during event 1, the perpendicular distance from the PDP to the flux tube of the electron beam was much greater than the 2 to 4 m predicted beam radius, so that the PDP was well outside of the region of the primary beam. Events 1 and 2 occur when the PDP was closest to the flux tube of the electron beam, and are the largest in magnitude.

The average potential measurements for events 1–5 are

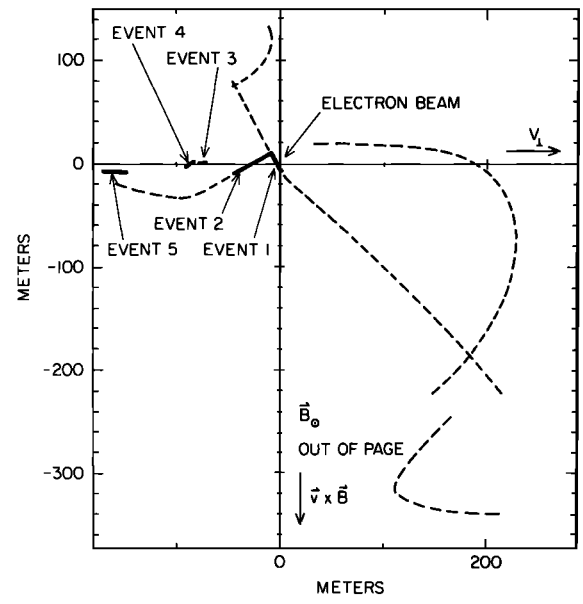

Fig. 3. Dashed lines indicate the trajectory of PDP in the plane perpendicular to **B** during times of electron beam generator operation. The trajectories for events 1–5 are shown as solid segments. The origin represents the position of the magnetic field line on which the beam lies. $V_\perp$ is the component of velocity perpendicular to **B**.

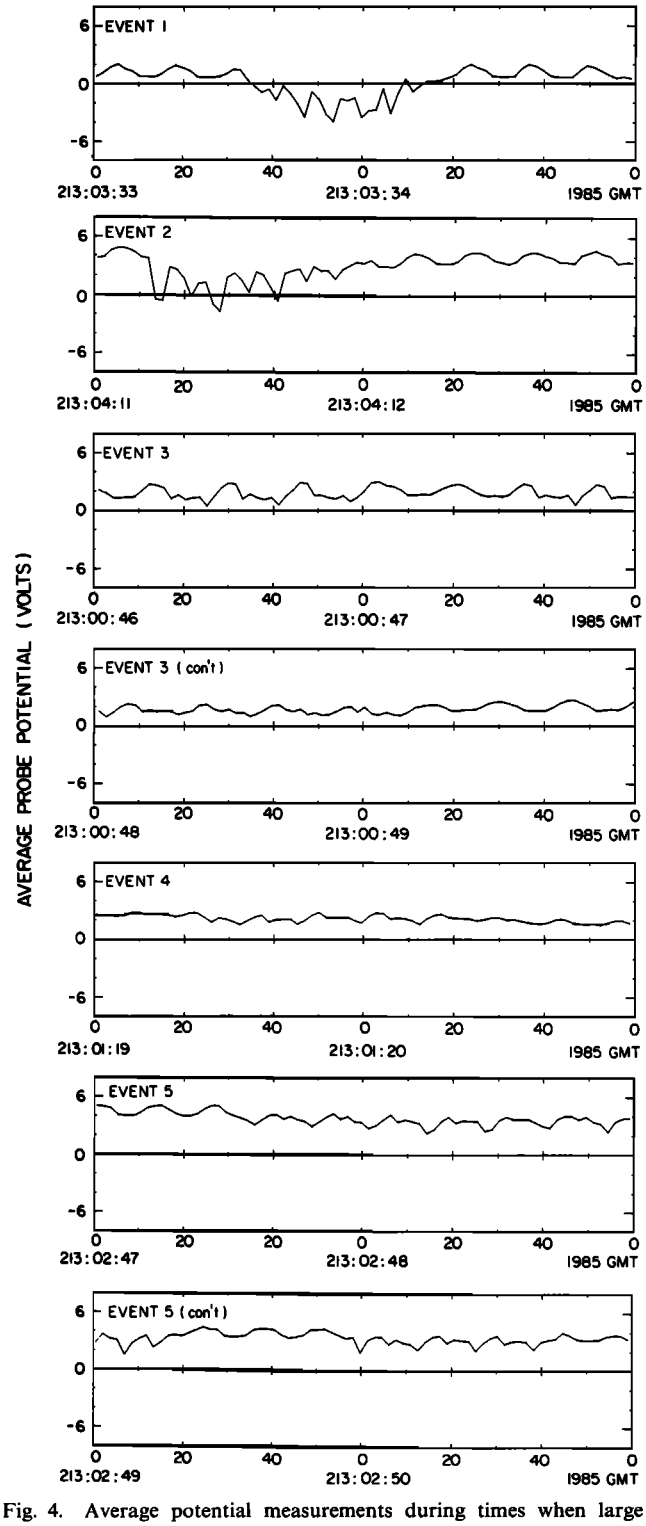

Fig. 4. Average potential measurements during times when large differential voltage signals were detected.

shown in Figure 4. The largest changes in the average potential measurements associated with the electron beam are seen during events 1 and 2, where the average potential of the probes goes from positive values of +2 to +4 V to negative values of −2 to −4 V. The spin period variation of the signal discussed above can be seen in the graphs for events 1 and 2 during the times before and after the large negative excursions of the signal. During events 3, 4, and 5, the average potential does not change by a large amount, but the smooth spin period variation of the signal is disrupted.

4. Interpretation

Because the determination of the quasi-static electric field with the PDP is based on measurements of the differential voltage between two floating probes, the results can be affected by energetic beam electrons striking the probes. It is easily shown that a small flux of energetic electrons may alter the floating potential of the probes by a large amount [*Fahleson*, 1967]. *Arnoldy and Winckler* [1981] reported a population of energetic electrons in the region around an electron beam, causing the floating potential of the Echo 3 rocket to become several volts negative. A similar observation was made on Echo 6 [*Winckler et al.* 1984]. Thus we might expect to find that the PDP potential is affected by energetic electrons around the beam. In fact, during each of events 1–5 discussed here, the LEPEDEA on the PDP detected energetic electrons at energies nearly up to the beam energy (W. R. Paterson, personal communication, 1987). Further, data from the PDP Langmuir probe seems to indicate that the PDP charged to at least −4.3 V during event 2, and to at least −7.6 V during event 1 (A. C. Tribble, personal communication, 1987). Therefore there is reason to suspect that the probes also charged. If the charging is different for the two probes, then V_{diff}/L cannot be safely interpreted as a good measure of the electric field.

To determine the possible effect of energetic electrons on our measurements, we perform a simple calculation of the floating potential. This is done by considering the balance of currents to the object of concern (see, for example, *Kasha* [1969]). The possible current sources are (1) thermal (background) electrons, (2) thermal (background) ions swept up by the motion of the spacecraft, (3) energetic electrons (energies $\gg kT_e$), (4) energetic ions (energies $\gg$ 5.0 eV, the ramming energy), (5) secondary electron emission, and (6) photoelectron emission. Measurements made with the LEPEDEA indicate that the current from energetic ions is much less than that from the ramming ions (W. R. Paterson, personal communication, 1987), so this current can be neglected. The maximum secondary electron yields for aluminum (PDP surface material) and graphite (probe surface material), are 1.0 secondaries/primary for 300-eV primaries [*Whetten*, 1985]. Thus secondary production would reduce the negative charging effect of the energetic electrons by some fraction. Photoemission would also reduce the negative charging. But since we wish to obtain a worst case estimate of the spacecraft potential, we neglect both secondary production and photoemission. We consider then the following current balance equation for an object at potential $V < 0$:

$$A_x n_e u_{sc}(1 - eV/E_i) - A_s n_e (kT_e/2\pi m_e)^{1/2} \exp(eV/kT_e) - A_s J_b = 0 \quad (1)$$

The first term in the above equation includes the ion current due to the sweeping up of the ionospheric ions by the spacecraft motion plus some effect of the attraction of ions to the negatively charged object. The second term is the electron current from the thermal electrons. The third term is the current to the object due to energetic electrons. The variables in (1) are identified in Table 3.

Using the representative parameters given in Table 3, equation (1) was solved numerically for various values of J_b and n_e. The floating potential was determined from (1) for both the

TABLE 3. Parameters Used in Evaluation of Equation (1)

	Value
U_{sc} spacecraft velocity	7.8×10^3 m/s
A_x cross-sectional area for ion collection:	
PDP	0.869 m^2
probe	8.11×10^{-3} m^2
A_s total surface area: PDP	4.52 m^2
probe	3.24×10^{-2} m^2
E_i ion energy in spacecraft reference frame	5.08 eV
T_e electron temperature	0.2 eV
n_e plasma density	5.0×10^{11} m^{-3}
J_b current density of energetic electrons	0–5.5×10^{-4} amp/m^2

spherical probes and for the PDP chassis. The current collecting area of the PDP was taken to be its surface area. Unfortunately, the current collecting properties of the spacecraft body are complicated, and this estimate is to be taken only as a rough approximation. The solution for the floating potential as a function of the energetic electron current density is plotted in Figure 5. Measurements from the LEPEDEA during beam event 1 indicate that J_b was as high as 4×10^{-4} amp/m^2 (W. R. Paterson, personal commuication, 1987). The Langmuir probe measurements indicate that during event 1, n_e was of the order of 1×10^{11} m^{-3} (A. C. Tribble, personal communication, 1987). From Figure 5 one can see that under the conditions of event 1 the PDP floating potential could easily be lower than -10 V. This is consistent with the Langmuir probe observation mentioned previously that the PDP charged to at least -7.6 V during event 1. More importantly for the V_{diff} measurements, under the conditions of event 1 differences in J_b on the order of 10^{-5} amp/m^2 lead to floating potential differences on the probes of several volts. During events 2, 3, 4, and 5 the Langmuir probe measurements indicate that n_e was of the order of 1×10^{10} m^{-3} (A. C. Tribble, personal communication, 1987). For this lower ambient density, Figure 5 shows that differences in J_b of the order of 10^{-6} amp/m^2 lead to floating potential differences on the probes of several volts. Figure 5 also shows that for a fixed value of J_b, small differences in the ambient plasma density lead to floating potential differences of several volts.

Using the differential voltage between the probes to infer electric field values can produce erroneous results if the two antenna probes receive different amounts of current from any of the various current sources. Current differences can occur if one of the probes is shielded by the PDP chassis from a current source, or if the plasma environment is nonuniform over the length of the antenna. During events 2, 3, 4, and 5 the peaks in V_{diff} are associated with specific orientations of the antenna with respect to the velocity and the magnetic field, and therefore can be primarily attributed to shadowing effects. Shadowing effects of this type were observed by *Winckler et al.* [1984] during the Echo 6 experiment. In that experiment, large signals at the payload spin frequency were attributed to shadowing of one probe from a magnetic field aligned plasma flow. At the time, the electric probes were stowed in the payload body. During events 3, 4, and 5 the "double peak" character of the signals indicates that two different shadowing effects are occurring. These two effects are discussed separately below.

For events 3, 4, and 5 one finds a voltage peak, and therefore a probable shadowing of one probe, when the antenna is aligned with the magnetic field projected onto the spin plane. Because the local ion larmor radius is much larger than the PDP, a shadowing along field lines suggests a shadowing of electrons. We explain the signal peak in the following manner. For events 3, 4, and 5 the beam was injected in the direction of **B**. At the time when the antenna was aligned with **B** in the spin plane, the probe on the boom pointing in the direction of **B** was at a lower potential than the probe on the boom pointing in the direction of $-$**B**. Thus we conclude that some energetic electrons are moving in the direction of $-$**B**, and one probe is shielded from them. So, for the three events when the PDP is 80 or more meters from the beam, the energetic elec-

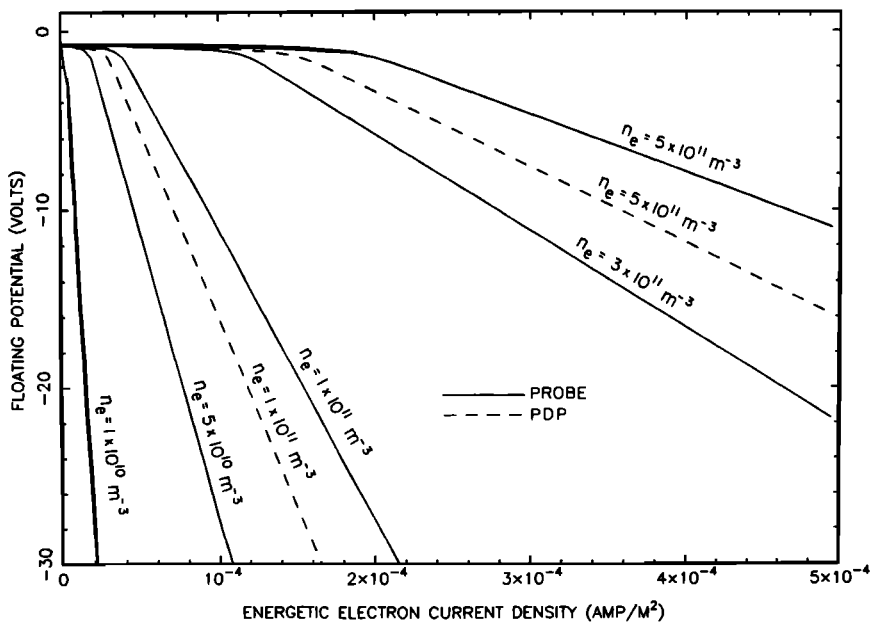

Fig. 5. Solution of equation (1) using values from Table 3. Model of floating potential as a function of energetic electron current. Antenna probe and PDP chassis have different floating potentials because of their different current collecting surface areas.

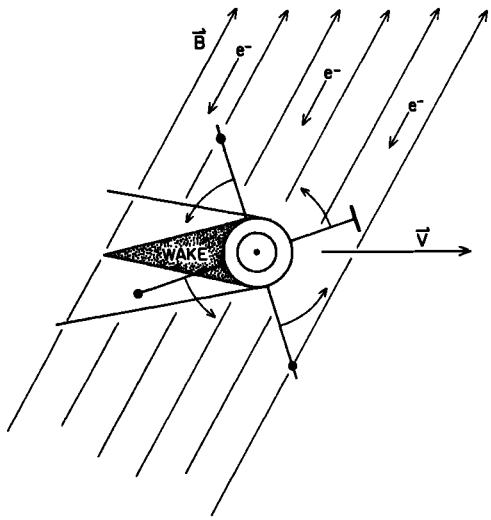

Fig. 6a. The PDP with the spin plane corresponding to the plane of the page. Energetic electrons move along the field lines. As the PDP spins, the antenna periodically becomes aligned with the magnetic field, and one probe is shielded from the electron flux. The probe also passes through the PDP wake.

trons have a preferred direction, which is opposite to the injection direction. This explanation is consistent with the report by the LEPEDEA group of a secondary electron beam in the shuttle wake [*Frank et al.*, 1987]. The shadowing of one probe from electrons moving down the field lines is pictured in Figure 6a. Consideration of Figure 6b shows that if the angle θ of the magnetic field to the spacecraft spin plane is too large, then shadowing along the field lines will not occur. The range of angles where shadowing is possible is $\theta < 20.4°$. Referring to the values of θ listed in Table 2, one finds that shadowing along field lines is possible for events 2, 3, 4, and 5.

The energetic electrons moving down the field lines and charging the probes in events 3, 4, and 5, may be attributed to reflection of beam electrons by collisions with atmospheric neutrals, or to a beam plasma interaction. First, consider reflection of electrons by collisions. Given the distance of the PDP downstream from the beam for these events, and the spacecraft velocity, one can determine the time of flight for the energetic electrons to be around 10 to 20 ms. For 1-keV electrons, the corresponding total distance traveled is about 200 to 400 km. For comparison, the mean free path of electrons for collisions with oxygen atoms can be roughly estimated by $\lambda = 1/(n_n\sigma)$, where n_n is the atomic oxygen density and σ is the collision cross section. We use a value for σ of 7×10^{-16} cm^2, the total scattering cross section for 100 eV electrons measured by *Sunshine et al.* [1967]. At an altitude of 300 km, n_n is approximately 10^8 cm^{-3} [*Johnson*, 1965], which yields a mean free path $\lambda \approx 140$ km. Because the atomic oxygen density is larger at lower altitudes, λ will become shorter at lower altitudes. Thus for events 1 and 3 where the beam was injected downward, it is quite reasonable that electrons reflected by collisions with neutrals could reach the PDP. Since the atomic oxygen density is smaller at higher altitudes, λ becomes longer at higher altitudes. At an altitude of 400 km, n_n is approximately 10^7 cm^{-3}, which yields $\lambda \approx 1400$ km. So for electrons injected upward, the effective mean free path will be $\gg 1400$ km. For events 2, 4, and 5 where the beam was injected upward, it may seem unlikely that the PDP could be affected by reflected electrons. However, it is not necessary that most of the beam particles be reflected. The solution of (1) showed that the measured signals are explained by differential energetic electron currents of the order of 10^{-6} amp/m^2, and this current can result from only a small percentage of beam particles being reflected. An alternative explanation for the presence of energetic electrons is considered by *Wilhelm et al.* [1985]. In the SCEX experiment, Wilhelm et al. measured energetic electrons in the region downstream of an electron beam. They discuss the possibility that the energetic electrons are the product of a beam plasma interaction. Both explanations are possible, and without a further more detailed analysis we cannot say which is correct.

A different shadowing effect occurs for events 2, 3, 4, and 5 when the antenna is aligned with the velocity vector. Because the local ion thermal speed is less than the spacecraft velocity, ions are swept up by the spacecraft motion. The electron thermal velocity is much greater than spacecraft velocity, so the electrons are not swept up. However, because quasi-neutrality must be maintained, both the ion and the electron densities are reduced behind the spacecraft, forming a plasma wake. The sweeping of the antenna through the wake as the PDP spins is indicated in Figure 6a. Because the velocity vector lies in the PDP spin plane as shown, the antenna always passes through the wake region. In order to estimate the plasma density in the wake at the location of the antenna probe, we use the self-similar solution for the expansion of a plasma into a vacuum as shown by *Samir et al.* [1983] and *Singh and Schunk* [1982]. In the standard treatment one assumes initially a plasma of density N_0 for the region $x < 0$, and a vacuum for the region $x > 0$. At time $t = 0$ the plasma is allowed to expand into the vacuum region. The solution for the density at later times is given by

$$N = N_0 \exp\left[\left(\frac{x}{S_0 t} + 1\right)\right] \tag{2}$$

where S_0 is the ion sound speed. To obtain an estimate of the density at the probe when the probe is in the wake, we use (2) and take for x the radius of the PDP, $x = 0.53$ m, and for t the time for the ionospheric plasma to flow a distance of half of the antenna length relative to the PDP, $t = 2.5 \times 10^{-4}$ s. Assuming an electron temperature of 0.2 eV, and assuming ions are atomic oxygen, the ion sound speed is estimated to be

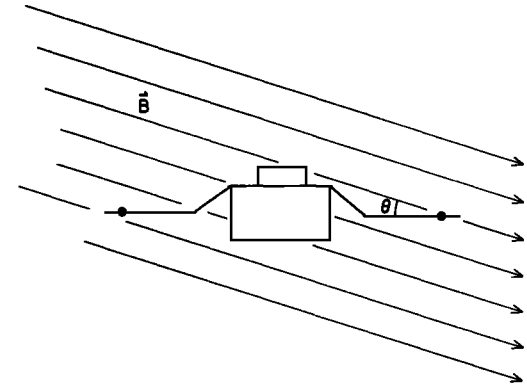

Fig. 6b. The PDP viewed with the spin axis in the plane of the page. The angle θ of the magnetic field to the spin plane is shown. If θ is small, then particles moving along field lines can be shadowed from one probe.

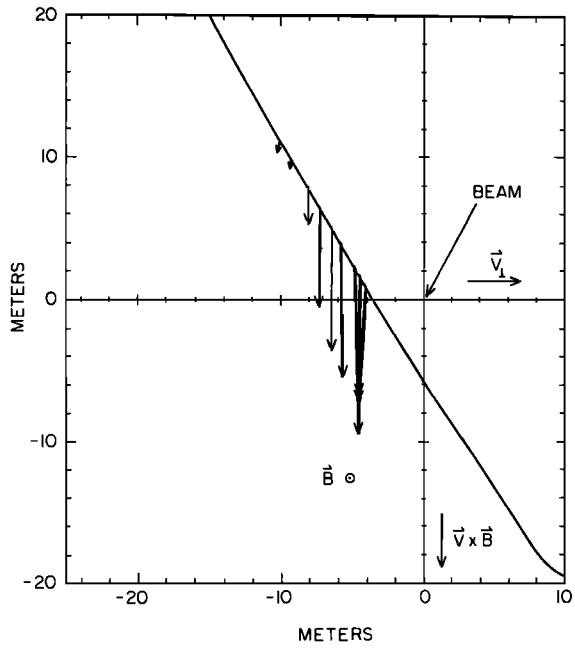

Fig. 7. Vectors showing the gradient in energetic electron flux along the trajectory of the PDP during event 1. Note that the beam will have a finite width, and the location of the beam center shown is accurate only to within a few meters.

about 1.4×10^3 m/s, yielding a wake density

$$N = 0.08N_0 \tag{3}$$

This solution corresponds to the expansion of the plasma in one direction only. The wake fills in from all directions, so we expect the density in the wake at the location of the antenna probe to be greater than 0.08 N_0, but still significantly less than N_0. Examination of Figure 5 shows that if both probes receive the same amount of energetic electron current, but one probe is in the wake where the density is lower, then the probe in the wake will be several volts lower in potential than the probe upstream. This explanation is consistent with the observed signals.

Event 1 does not lend itself to explanation in terms of probe shadowing, as the other events do. The angle θ between the magnetic field and the spin plane (see Table 2) is greater than 20.4°, so that probes are not shadowed along field lines. Figure 2 shows that the peaks in voltage are not consistently centered about the times the antenna is aligned with the velocity vector or the magnetic field. The peaks are also broader than expected if due only to a shielding effect. Thus the signal is due either to a gradient in the fluxes of energetic electrons reaching the probes, or both a gradient in fluxes of energetic electrons and an electric field. We cannot rule out the possibility that we have measured the electric field. However, because the entire region where the large electric field signals and the energetic electrons are observed is only 20 meters wide (refer to Figure 3), gradients over the antenna length are expected. As will be discussed below, we consider it likely that the large V_{diff} signal in event 1 is caused mainly by a gradient in energetic electron fluxes.

In order to investigate the possible interpretation of the large signals associated with event 1, the V_{diff} signals were analyzed as follows. Due to the spacecraft rotation, the V_{diff} signal varies sinusoidally with the PDP spin period of 13.1 s, and we assume that V_{diff} attains peak value when the antenna is aligned with the direction of strongest gradient in the energetic electrons. The direction and relative magnitude of the gradient is then obtained by using a least squares method to fit a 13.1-s segment of the V_{diff} signal to the function

$$F(t) = F_1 + F_2 \cos(2\pi t/T - \Phi) \tag{4}$$

where $T = 13.1$ s, and F_1, F_2, and Φ are parameters determined by the fit procedure. If the signal is interpreted as a measure of the gradient of the energetic electron flux, then the constant F_2 gives the magnitude of the gradient and Φ gives the direction of the gradient in the spin plane. We do not expect the energetic electron flux to vary much along the direction of **B**, so we assume that the gradient lies in the plane perpendicular to **B** and that we have measured the component of the gradient projected onto the PDP spin plane. Using this assumption, the magnitude of the gradient vector in the plane perpendicular to **B** was determined. In order to establish a "goodness of fit" of the curve fit performed for each measurement, the following test variable was calculated:

$$X = [\textstyle\sum (F(t_i) - x_i)^2/(N-3)]^{1/2}/F_2 \tag{5}$$

where x_i is the V_{diff} signal at time t_i, and N is the number of sample points used in one curve fit. Measurements were retained if $X < 0.25$, corresponding roughly to 25% error.

The vectors obtained by the above analysis are shown in Figure 7. The vectors are plotted along the trajectory of the PDP relative to the electron beam where the coordinate directions are the same as in Figure 3. The V_{diff} signals first becomes larger than $|(\mathbf{V} \times \mathbf{B}) \cdot \mathbf{L}|$, and the gradient in the energetic electron flux first becomes significant, when the PDP is about 10 m away from a line extending directly downstream from the center of the beam. The V_{diff} signal, and thus the gradient in the electron flux, become larger as the PDP gets closer to this line. The gradient vectors tend to point toward the line. The indicated picture is that of a region of energetic electrons downstream from the primary electron beam. The region is not homogeneous but rather the electron flux is peaked along the line extending directly downstream from the primary beam.

The presence of a gradient in energetic electron flux can account for the large magnitude (larger than 8 V) of the V_{diff} signals during event 1. If the magnitude of the gradient in J_b is estimated from the LEPEDEA measurements, then the V_{diff} signal that would result from such a gradient can be estimated. As stated previously, the LEPEDEA measured a peak value of J_b of about 4×10^{-4} amp/m^2. We assume that the flux of energetic electrons is peaked on a line extending directly downstream from the center of the beam, and is symmetric about that line. Since the region where large signals are detected is about 20 m wide, the spatial gradient $\Delta J_b/\Delta x$ is approximately $(4 \times 10^{-4}$ amp/m$^2)/(10$ m$) = 4 \times 10^{-5}$ amp/m. The resulting V_{diff} can be estimated by

$$V_{\text{diff}} = (\Delta J_b/\Delta x)(\Delta V/\Delta J_b)(L \sin\theta) \tag{6}$$

where the quantity $\Delta V/\Delta J_b$ must be determined from Figure 5, L is the antenna length, and θ is the angle of **B** to the spin plane. For $n_{e^-} = 1 \times 10^{11}$ m^{-3} and $J_b > 4 \times 10^{-5}$ amp/m^2, $\Delta V/\Delta J_b$ is -1.6×10^5 V/amp/m^2. The antenna length is 3.89 m (see Table 1) and Θ is about 23° (see Table 2). Using equation (4) with the given values, we obtain $V_{\text{diff}} \approx 9.7$ V. Thus a gradient in the energetic electron flux of the magnitude indicated by the LEPEDEA measurements could easily produce the V_{diff} signals recorded during event 1.

Analysis of all five events suggests that energetic electrons are found in a region about 20 m wide extending up to 170 m downstream from the injected electron beam. Consideration of event 1 indicates that very close to the beam, there is a large spatial gradient in the energetic electron flux: the flux increases as one approaches the line extending directly downstream from the center of the beam. We expect that the energetic electron flux is symmetric about this line. For events 3, 4, and 5, in which the PDP was 80 or more meters away from the beam, the signals are explained by the presence of energetic electrons having a preferential direction of motion along the magnetic field line, but in a direction opposite to the beam injection.

Although the main features of the V_{diff} signals during events 1–5 are understood in terms of the discussion given above, some features remain unexplained. For example, the voltage peaks during event 4 are bumps on a signal that is otherwise sinusoidal. The peaks in event 4 are explained by alignment of the antenna with the magnetic field or with the velocity vector in the presence of energetic electrons. However, the V_{diff} signal for event 4 shown in Figure 2 would also provide a reasonably good fit to the function in (4). Yet, since the shadowing effects are apparent in the measurements, a fit of the signal to (4) would be difficult to interpret. It is not clear why event 4 has a more sinusoidal character than events 3 or 5. Similarly, the large peaks in the signal during event 2 can be attributed to alignment of the antenna with the velocity vector in the presence of energetic electrons, but the signal remains $> |(\mathbf{V} \times \mathbf{B}) \cdot \mathbf{L}|$ when the probes are not in the spacecraft wake.

Finally, we consider the average potential measurements. The measurements show that during periods of no beam operation, the average probe floating potential was several volts higher than the PDP chassis floating potential. The solution of (1) (see Figure 5) indicates that the probes should float to a potential which is much less than a volt higher than the PDP potential. During events 1 and 2 the average probe floating potential became lower than the PDP potential. The solution of (1) indicates that the average probe floating potential should always be higher than the PDP chassis potential. The reasons for these discrepancies are not clear. However, we speculate that explanation involves the properties of the PDP surface materials. In solving (1) for the PDP potential, we assumed the PDP to have a uniformly conducting surface. However the potential of the aluminum mesh on the PDP surface may be influenced by the fiberglass cloth which underlies it. The fiberglass cloth may be charging to a different potential than the aluminum mesh. *Katz and Davis* [1987] analyze some of the effects of the fiberglass cloth-aluminum mesh arrangement for the situation of the PDP attached to the shuttle. The ultimate effect on the mesh potential for the PDP in free flight is uncertain.

5. Conclusions

Our conclusion from this analysis is that the large signals measured by the PDP quasi-static electric field instrument during electron beam operation can primarily be attributed to three causes. First, at times when the electric antenna is aligned with the projection of the magnetic field into the spin plane, the spacecraft body shields one probe from energetic electrons moving along the magnetic field lines. The two probes receive different amounts of electron current, thereby causing large signals. Second, at times when energetic electrons are reaching both probes, but one probe is in the PDP wake, the wake produces asymmetries in the plasma density at the two probes, thereby causing large signals. Finally, spatial gradients in the energetic electron fluxes between the two antenna probes produce differences in the energetic electron current to the two probes, thereby causing large signals. When the electron beam generator is operating, energetic electrons are found in a region about 20 m wide and up to 170 m downstream from the injected electron beam. Because the region is so narrow, the spatial gradients are significant even over the length of the PDP antenna. For events 80 or more meters away from the beam, the electric field results are explained by the presence of energetic electrons having a preferential motion back down the magnetic field line on which the beam was injected.

On the Spacelab 2 mission, it was demonstrated that with the shuttle it is possible to carry out detailed studies of electron beam effects under carefully controlled conditions. Thus, it should be possible to obtain a good map of the electric field near an electron beam. However, our experience indicates that double probe floating potential measurements are not reliable in the region near the beam. The floating potential of an object in a region with substantial fluxes of energetic electrons can be many times kT_e/e more negative than the plasma potential. A small difference in energetic electron current collected by each probe of a double probe system can then lead to differential voltages much higher than those due to any electric field in the plasma. Reliable potential measurements probably will require biased probes, such as described by *Fahleson* [1967], or emissive probes such as described by *Bettinger* [1965]. These active potential measurements are not as sensitive to energetic electrons. An example of a biased probe system is found on the ISEE-1 spacecraft [*Mozer et al.*, 1978]. In general, though, active potential measurements have not been widely used because of the appealing simplicity of floating potential measurements. However, for future spacecraft electron beam experiments, active instead of passive potential measurements will probably have to be considered.

Acknowledgments. The authors thank Louis A. Frank and William R. Paterson for the use of the LEPEDEA measurements, and for their help. We thank Nicola D'Angelo for use of the Langmuir probe measurements. We also acknowledge the useful discussions with Rock Bush, William M. Farrell, Karl Lonngren, Gerald B. Murphy, Jolene S. Pickett and Alan C. Tribble. This research was supported by NASA through contract NAS8-32807 with Marshall Space Flight Center, contract NAG3-449 with the Lewis Research Center, and grant NGL 16-001-043 with NASA Headquarters.

The Editor thanks B. A. Whalen and J. R. Winckler for their assistance in evaluating this paper.

References

Arnoldy, R. L., and J. R. Winckler, The hot plasma environment and floating potentials of an electron beam-emitting rocket in the ionosphere, *J. Geophys. Res.*, *86*, 575–584, 1981.

Banks, P. M., W. J. Raitt, A. B. White, R. I. Bush, and P. R. Williams, Results from the Vehicle Charging and Potential Experiment on STS-3, *J. Spacecr. Rockets*, *28*, 138–149, 1987.

Bettinger, R. T., An in situ probe system for measurement of ionospheric parameters, in *Interactions of Space Vehicles With an Ionized Atmosphere*, edited by S. F. Singer, pp. 163–270, Pergamon, New York, 1965.

Denig, W. F., Wave and particle observations associated with the beam plasma discharge in a space simulation chamber, Ph.D. thesis, Utah State Univ., Logan, 1982.

Fahleson, U., Theory of electric field measurements conducted in the magnetosphere with electric probes, *Space Sci. Rev.*, *7*, 238–262, 1967.

Frank, L. A., D. A. Gurnett, M. Ashour-Abdalla, W. R. Paterson,

W. S. Kurth, N. Omidi, P. M. Banks, and W. J. Raitt, The secondary electron beams and plasma waves associated with electron beam injection in space (abstract), *Bull. Am. Phys. Soc.*, *32*, 1823, 1987.

Jacobsen, T. A., and N. C. Maynard, Polar 5—An electron acceleration experiment within an aurora, 3, Evidence for significant spacecraft charging by an electron accelerator at ionospheric altitude, *Planet. Space Sci.*, *28*, 291–307, 1978.

Johnson, F. S., Structure of the upper atmosphere, in *Satellite Environment Handbook*, edited by F. S. Johnson, pp. 3–20, Stanford University Press, Stanford, Calif., 1965.

Kasha, M. A., *The Ionosphere and Its Interaction With Satellites*, Gordon and Breach, New York, 1969.

Katz, I., and V. A. Davis, Ram ion scattering caused by space shuttle $\mathbf{V} \times \mathbf{B}$ induced differential charging, *J. Geophys. Res.*, *92*, 8787–8791, 1987.

Kellogg, P. J., H. R. Anderson, W. Bernstein, T. J. Hallinan, R. H. Holzworth, R. J. Jost, H. Leinbach, and E. P. Szuszczewicz, Laboratory simulation of injection particle beams in the ionosphere, in *Artificial Particle Beams in Space Plasma Studies*, edited by B. Grandel, p. 289, Plenum, New York, 1982.

Mozer, F. S., R. B. Torbert, U. V. Fahleson, C. G. Falthammer, A. Gonfalalone, and A. Pedersen, Measurements of quasi-static and low-frequency electric fields with spherical double probes on the ISEE-1 spacecraft, *IEEE Trans. Geosci. Electron.*, *GE-16*, 258–261, 1978.

Samir, U., K. H. Wright, Jr., and N. H. Stone, The expansion of a plasma into a vacuum: Basic phenomena and processes and applications to space plasma physics, *Rev. Geophys.*, *21*, 1631, 1983.

Shawhan, S. D., Description of the plasma diagnostics package (PDP) for the OSS-1 shuttle mission and JSC chamber test in conjunction with the fast pulse electron gun (FPEG), in *Artificial Particle Beams in Space Studies*, edited by B. Grandel, pp. 419–430, Plenum, New York, 1982.

Shawhan, S. D., G. B. Murphy, P. M. Banks, P. R. Williamson, and W. J. Raitt, Wave emissions from dc and modulated electron beams on STS-3, *Radio Sci.*, *19*, 471–486, 1984.

Singh, N., and R. W. Schunk, Numerical calculations relevant to the initial expansion of the polar wind, *J. Geophys. Res.*, *87*, 9154, 1982.

Sunshine, G., B. B. Aubrey, and B. Bederson, Absolute measurements of total cross sections for the scattering of low-energy electrons by atomic and molecular oxygen, *Phys. Rev.*, *154*, 1–8, 1967.

Tribble, A. C., N. D'Angelo, G. Murphy, J. Pickett, and J. T. Steinberg, Exposed high-voltage source effect on the potential of an ionospheric satellite, *J. Spacecr. Rockets*, *25*, 64–69, 1988.

Whetten, N. R., Secondary electron emission, in *CRC Handbook of Chemistry and Physics*, 65th ed., CRC Press, Boca Raton, Fla., 1985.

Wilhelm, K., W. Bernstein, P. J. Kellogg, and B. A. Whalen, Fast magnetospheric echoes of energetic electron beams, *J. Geophys. Res.*, *90*, 491–504, 1985.

Winckler, J. R., and K. N. Erickson, Plasma heating, plasma flow and wave production around an electron beam injected into the ionosphere, JPL Symposium on Space Technology Plasma Issues in 2001, edited by H. Garrett, J. Feynman, and S. Gabriel, *JPL Publ.*, *86-49*, 295–306, Oct. 1, 1986.

Winckler, J. R., J. E. Steffen, P. R. Malcolm, K. N. Erickson, Y. Abe, and R. L. Swanson, Ion resonances and ELF wave production by an electron beam injected into the ionosphere: Echo 6, *J. Geophys. Res.*, *89*, 7565–7571, 1984.

P. M. Banks, STAR Laboratory, Stanford University, Stanford, CA 94305.

D. A. Gurnett, Department of Physics and Astronomy, University of Iowa, Iowa City, IA 52242.

J. T. Steinberg, Center for Space Research, Massachusetts Institute of Technology, Cambridge, MA 02139.

(Received July 28, 1987;
revised April 22, 1988;
accepted May 26, 1988.)